Inorg. Chem. **2003**, *42*, 1316–1321

Metal-Dependent Ferro- Versus Antiferromagnetic Interactions in Molecular Crystals of Square Planar {M(II) Imino-Nitroxide Radical} Complexes (M = Pt, Pd)

Mohammed Fettouhi,*,† Bassam El Ali,† Mohammed Morsy,† Stéphane Golhen,‡ Lahcène Ouahab,*,‡ Boris Le Guennic,‡ Jean-Yves Saillard,‡ Nathalie Daro,§ Jean-Pascal Sutter,*,§ and Edmond Amouyal||

Chemistry Department, King Fahd University of Petroleum and Minerals, Po Box 5048, Dhahran 31261, Saudi Arabia, Laboratoire de Chimie du Solide et Inorganique Moléculaire, UMR 6511 CNRS Université de Rennes 1, Institut de Chimie de Rennes, Avenue du Général Leclerc, 35042 Rennes Cedex, France, Institut de Chimie de la Matière Condensée de Bordeaux, CNRS UPR 9048, 33608 Pessac, France, and Laboratoire de Chimie Physique, CNRS UMR 8000, Université Paris-Sud, Bâtiment 350, F-91405 Orsay, France

Received March 11, 2002

The synthesis and structural, spectral, and magnetic characterizations of two new complexes of formula [Pt(IM_2-Py)Cl_2] (**A**) and [Pd(IM_2Py)Cl_2] (**B**) are reported. IM_2Py stands for the imino-nitroxide radical ligand 2-(ortho-pyridyl)-4,4,5,5-tetramethylimidazoline-1-oxyl. Their crystal structures were solved at room temperature and at 120 K revealing structural phase transitions from pseudo-orthorhombic to monoclinic systems for the two compounds which remain isostructural in the whole temperature range explored. Structural parameters for **A**: $T = 293$ K [120 K], monoclinic ($P2_1/n$) [$P2_1/c$], $a = 7.906(2)$ [7.989(3)] Å, $b = 17.872(9)$ [10.168(4)] Å, $c = 10.357(3)$ [17.623(6)] Å, $\beta = 90.732(13)°$ [95.940(2)]°, $Z = 4$ [4]. Structural parameters for **B**: $T = 293$ K [120 K], monoclinic ($P2_1/n$) [$P2_1/c$], $a = 7.900(3)$ [7.9730(2)] Å, $b = 17.907(9)$ [10.1806(3)] Å, $c = 10.299(3)$ [17.7171(4)] Å, $\beta = 90.524(14)°$ [95.747(2)]°, $Z = 4$ [4]. In both complexes, the metal coordination is essentially planar. The average Pt–N, Pt–Cl and Pd–N, Pd–Cl bond lengths are 1.996(6) [1.88], 2.295(2) [2.248(8)] Å and 2.015(7) [2.029(8)], 2.287(3) [2.294(3)] Å, respectively. The solid state structure is characterized by a pairlike molecular packing stacked in columns parallel to the *a* axis; this dimer character is reinforced at low temperature. Despite their structural similarity, the investigation of the magnetic properties revealed that dominant ferromagnetic interactions govern the behavior of the Pt derivative **A**, whereas antiferromagnetic interactions take place for the Pd compound **B**. A rationalization for this rather intriguing difference is proposed in light of the spin population deduced from density functional theory calculations. The electronic absorption spectra of **A** and **B** present structured absorption bands in the visible which are attributed to MLCT transitions. Both compounds are nonluminescent at room temperature. However, a weak emission is detected for **A** in butyronitrile glasses at 77 K, indicating that the MLCT excited state is strongly quenched at low temperature.

Introduction:

Molecular magnetic materials have attracted an increasing interest during the last two decades because of their potential application in future devices.[1−6] Among the synthetic strategies adopted, coordination chemistry stands as a powerful tool for the design of such materials. The systems achieved

* Authors to whom correspondence should be addressed. E-mail: ouahab@univ-rennes1.fr (L.O); fettouhi@kfupm.edu.sa (M.F.); psutter@icmcb.u-bordeaux.fr (J.-P.S.).
† King Fahd University of Petroleum and Minerals.
‡ Institut de Chimie de Rennes.
§ Institut de Chimie de la Matière Condensée de Bordeaux.
|| Université Paris-Sud.

(1) *Magnetism: Molecules to Materials*; Miller, J. S, Drillon, M., Eds.; Wiley-VCH: New York, 2001.
(2) Itoh, K.; Kinoshita, M. *Molecular Magnetism, New Magnetic Materials*; Kodansha & Gordon and Breach: Langhorne, PA, 2000.
(3) Kahn, O. *Molecular Magnetism*; VCH: New York, 1993.
(4) Ouahab, L. *Chem. Mater.* **1997**, *9*, 1909 and references therein.
(5) Miller, J. S.; Epstein, A. J. *Angew. Chem., Int. Ed. Engl.* **1994**, *33*, 385 and references therein.
(6) Enoki. T.; Yamaura, J.-I.; Miyazaki, A. *Bull. Chem. Soc. Jpn.* **1997**, *70*, 2005 and references therein.

10.1021/ic0255813 CCC: $25.00
Published on Web 01/17/2003

vary from discrete molecules to 1D chains, and 2D and 3D networks.[1−9] For the materials made up from discrete molecules, it is usually rather difficult to gain control over the molecular packing. Nevertheless, molecular planarity as a geometrical criterion was shown to be of great importance. This fact is exemplified by the first molecular ferromagnet, $Fe(Cp^*)_2TCNE$.[10] In this context, the coordination chemistry of nitronyl nitroxide radical based ligands afforded, in addition to few 1D and 2D systems, a large number of discrete molecule species.[11−23] Taking into account the planarity criterion, the coordination chemistry of group 10 metals represents the model system of choice when these metals are coupled to conjugated chelating ligands bearing a nitroxyl radical. Another attracting feature is the possibility of synergy between the optical properties of the complex and magnetic properties as encountered in the recently reported photosensitive magnets.[6−7,24−25] These metals fit this objective owing to their potential photophysical properties, namely luminescence. Indeed, square planar complexes are known to have emissive excited states in particular heteroaromatic chelates such as $Pt(bpy)Cl_2$ (bpy = 2,2′-bipyridine),[26] which has a structural similarity with the new compounds reported herein. Along this line, we have investigated the coordination chemistry of the ligand 2-(ortho-pyridyl)-4,4,5,5-tetramethylimidazoline-1-oxyl (IM_2Py) with MCl_2 precursors (M = Pd(II), Pt(II)) (Scheme 1). Two new complexes have hence been isolated. We report herein the synthesis, the X-ray single-crystal structures at room temperature and at low temperature, the spectral properties, the spin population deduced from the density functional theory calculations, and the magnetic characteristics of the two compounds $Pd(IM_2Py)Cl_2$ (**A**) and $Pt(IM_2Py)Cl_2$ (**B**).

Scheme 1

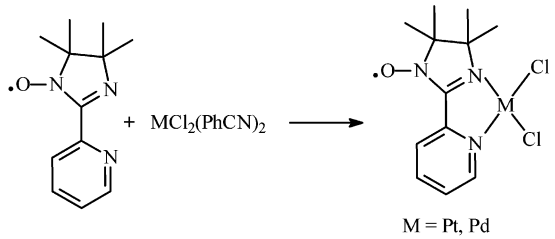

Experimental Section:

Syntheses. 2-(*ortho*-Pyridyl)-4,4,5,5-tetramethylimidazoline-1-oxyl[27] and dichlorobis(benzonitrile)M(II) (M = Pd, Pt)[28] were synthesized following literature procedures.

$Pt(IM_2Py)Cl_2$ (A). $PtCl_2(PhCN)_2$ (2.4 g; 5 mmol) and IM_2Py (2 g; 9 mmol) were reacted in 50 mL of dimethylformamide at room temperature. After 4 h of stirring, the mixture was filtered and the solvent removed under vacuum. The residue was washed thoroughly with acetone and air-dried. The product was recrystallized from dimethylformamide. Anal. Obsd (Calcd) for $PtN_3C_{12}H_{16}OCl_2$: C 29.70 (29.75); H 3.20 (3.30); N 8.66 (8.68). IR (KBr): 2986 (m), 2930 (m), 1612 (m), 1480 (s), 1456 (s), 1428 (s), 1376 (s), 1346 (s), 1256 (m), 1212 (m), 1144 (s), 1098 (m), 1060 (m), 778 (s), 746 (m), 652 (s) cm^{-1}.

$Pd(IM_2Py)Cl_2$ (B). $PdCl_2(PhCN)_2$ (1.9 g; 5 mmol) and IM_2Py (2 g; 9 mmol) were reacted in 50 mL of acetone at room temperature. After 2 h of stirring, the brown precipitate was collected by filtration, washed thoroughly with acetone, and air-dried. Recrystallization from dimethylformamide afforded parallelepipedic brown crystals. Anal. Obsd (Calcd) for $PdN_3C_{12}H_{16}OCl_2$: C 36.60 (36.42); H 4.19 (4.05); N 10.58 (10.62). IR (KBr): 2986 (m), 2930 (m), 1610 (m), 1540 (m), 1488 (m), 1454 (s), 1374 (m), 1352 (s), 1268 (m), 1205 (m), 1142 (s), 1096 (m), 780 (s), 744 (m), 654 (s) cm^{-1}.

Spectral and Magnetic Measurements. The IR spectra were recorded from KBr pellets on a Perkin-Elmer FTIR spectrophotometer (16F PC). The UV−vis electronic absorption spectra were recorded on a Perkin-Elmer Lambda 9 spectrophotometer. The emission spectra were obtained with a Jobin Yvon Spex Fluorolog FL 111 spectrofluorimeter. All luminescence measurements were made with deoxygenated solutions, in various solvents at room temperature and in butyronitrile at 77 K. At low temperature, we used cylindrical cells, and the solutions were cooled in a quartz Dewar containing liquid nitrogen. Some luminescence experiments in the solid phase were carried out with a laser flash photolysis setup using an excimer laser (Lambda Physik EMG 100, 308 nm pulses of 10 ns duration) as excitation source.[29] Spectroscopic grade solvents were used as supplied.

Magnetic measurements were carried out on a Quantum Design SQUID SPMS-5S magnetometer. The temperature dependence of the molar magnetic susceptibility, χ_M, for compounds **A** and **B** was measured in the temperature range 2−300 K, with an applied field of 1000 Oe. Data were corrected for the contribution of the sample holder, and diamagnetic contributions were estimated from Pascal's constants.

(7) Sato, O.; Iyoda, T.; Fujishima, A.; Hashimoto, K. *Science* **1996**, *272*, 704.
(8) Ohkoshi, S.; Fujishima, A.; Hashimoto, K. *J. Am. Chem. Soc.* **1998**, *120*, 5349.
(9) Mathonière, C.; Sutter, J.-P.; Yakhmi, J. V. In *Magnetism: molecules to materials*; Miller, J. S., Drillon, M., Eds.; Wiley-VCH: Weinheim, 2002; Vol. 4.
(10) Miller, J. S.; Epstein, A. J.; Reiff, W. M. *Science* **1988**, *240*, 40.
(11) Inoue, K.; Hayamizu, T.; Iwamura, H.; Hashizume, D.; Ohashi Y. *J. Am. Chem. Soc.* **1996**, *118*, 1803.
(12) Caneschi, A.; Gatteschi D.; Sessoli, R.; Rey, P. *Acc. Chem. Res.* **1989**, *22*, 392.
(13) Fegy, K.; Luneau, D.; Belorizky, E.; Novac, M.; Tholence, J. L.; Paulsen, C.; Ohm, T.; Rey, P. *Inorg. Chem.* **1998**, *37*, 4524.
(14) Caneschi, A.; Ferraro, F.; Gatteschi, D.; Rey, P.; Sessoli, R. *Inorg. Chem.* **1990**, *29*, 4217.
(15) Luneau, D.; Risoan, G.; Rey, P.; Grand, A.; Caneschi, A.; Gatteschi, D.; Laugier, J. *Inorg. Chem.* **1993**, *32*, 5616.
(16) Sayama, Y.; Handa, M.; Mikuriya, M.; Hiromitsu, I.; Kasuga, K. *Chem. Lett.* **1998**, 777.
(17) Huang, C. F.; Wei, H. H.; Lee, G. H.; Wang, Y. *Inorg. Chim. Acta*. **1998**, *279*, 233.
(18) Fettouhi, M.; Khaled, M.; Waheed, A.; Golhen, S.; Ouahab, L.; Sutter, J.-P.; Kahn. O. *Inorg, Chem.* **1999**, *38*, 3967.
(19) Dasna, I.; Golhen, S.; Ouahab, L.; Peña, O.; Guillevic, J.; Fettouhi, M. *J. Chem. Soc., Dalton Trans.* **2000**, 129.
(20) Cogne, A.; Laugier, J.; Luneau, D.; Rey, P. *Inorg. Chem.* **2000**, *39*, 5510.
(21) Dasna, I.; Golhen, S.; Ouahab, L.; Pena, O.; Daro, N.; Sutter, J. P. *C. R. Acad. Sci., Ser. IIc: Chim.* **2001**, *4*, 125.
(22) Daro, N.; Guionneau, P.; Golhen, S.; Chasseau, D.; Ouahab, L.; Sutter, J.-P. *Inorg. Chim. Acta* **2001**, *326*, 47.
(23) Rancurel, C.; Leznoff, D. B.; Sutter, J.-P.; Guionneau, P.; Chasseau, D.; Kliava, J.; Kahn, O. *Inorg. Chem.* **2000**, *39*, 1602.
(24) Escax, V.; Bleuzen, A.; Cartier dit Moulin, C.; Villain, F.; Goujon, A.; Varret, F.; Verdaguer, M. *J. Am. Chem. Soc.* **2001**, *123*, 12536 and references therein.
(25) Turner, S. S.; Michaut, C.; Kahn, O.; Ouahab, L.; Lecas, A.; Amouyal, E. *New J. Chem.* **1995**, *19*, 773.
(26) Miskowski, V. M.; Houlding, V. H. *Inorg, Chem.* **1989**, *28*, 1529.
(27) Ullman, E. F.; Call, L.; Osiecki, J. H. *J. Org. Chem.* **1970**, *35*, 3623.
(28) Evans, D.; Osborn, J. A.; Wilkinson, G. *Inorg. Synth.* **1968**, *11*, 99.
(29) Amouyal, E.; Mouallem-Bahout, M. *J. Chem. Soc., Dalton Trans.* **1992**, 509.

Table 1. Crystallographic Data for Compounds **A** and **B**

	A		**B**	
	293 K	120 K	293 K	120 K
formula	$C_{12}H_{16}Cl_2N_3OPt$		$C_{12}H_{16}Cl_2N_3OPd$	
fw	484.27		395.58	
cryst syst	monoclinic	monoclinic	monoclinic	monoclinic
space group	$P2_1/n$	$P2_1/c$	$P2_1/n$	$P2_1/c$
λ (Å)	0.71073	0.71073	0.71073	0.71073
a (Å)	7.906(2)	7.983(3)	7.900(3)	7.9730(2)
b (Å)	17.872(9)	10.168(4)	17.907(9)	10.1806(3)
c (Å)	10.357(3)	17.623(9)	10.299(3)	17.7171(4)
β (deg)	90.732(13)	95.940(2)	90.524(14)	95.747(2)
V (Å^3)	1463.3(9)	1423.8(9)	1457.0(10)	1430.87(6)
Z	4	4	4	4
ρ (g·cm^{-3})	2.198	2.259	1.803	1.836
indices for $[I > 2\sigma(I)]$	2406	2681	2237	3044
R1[a]	0.0381	0.1175	0.0689	0.0738
wR2[b]	0.0870	0.3367	0.1856	0.1852

[a] $R1 = \sum||F_o| - |F_c||/\sum|F_o|$. [b] $wR2 = \{\sum[w(F_o^2 - F_c^2)^2]/\sum[w(F_o^2)^2]\}^{1/2}$.

Table 2. Selected Bond Lengths (Å) and Bond Angles (deg) for **A** and **B** at 293 K and 120 K

	A, M = Pt		**B**, M = Pd	
	293 K	120 K	293 K	120 K
M−N(2)	1.995(5)	1.761(13)	2.015(6)	2.019(7)
M−N(1)	1.996(6)	2.01(2)	2.042(7)	2.039(8)
M−Cl(1)	2.288(2)	2.209(8)	2.263(2)	2.283(2)
M−Cl(2)	2.303(2)	2.287(6)	2.311(2)	2.306(2)
N(3)−O(1)	1.278(6)	1.27(2)	1.265(8)	1.269(10)
N(2)−M−N(1)	79.4(2)	81.1(6)	79.9(2)	79.8(3)
N(2)−M−Cl(1)	98.29(15)	97.8(4)	97.88(16)	97.1(2)
Cl(1)−M−Cl(2)	87.52(7)	87.2(2)	87.95(9)	88.06(8)
N(1)−M−Cl(2)	94.81(16)	94.0(6)	94.30(19)	94.94(19)

X-ray Data Collection and Structure Determination. Crystals were mounted on an Enraf-Nonius CAD4 diffractometer equipped with a graphite monochromatized Mo Kα radiation ($\lambda = 0.71073$ Å). At 293 K, the unit cell parameters were obtained by least-squares fits of the automatically centered 25 reflections. Intensity data were corrected for Lorentz and polarization effects. Data reduction and absorption correction, using the ψ-scan method, were performed with MolEN programs.[30] Low temperature (120 K) data were collected on an Enraf-Nonius four circle diffractometer equipped with a CCD camera and a graphite-monochromated Mo Kα radiation source ($\lambda = 0.71073$ Å). Structure solution and refinements were conducted with SHELXS-86 and SHELXL-97, respectively.[31−32] We can notice that, despite several data collections performed for **A** at low temperature, the refinements yielded high reliability factors. Crystallographic data are given in Table 1. Hydrogen atoms were included at calculated positions with isotropic thermal parameters proportional to those of the connected carbon atoms. Selected bond lengths and angles are given in Table 2. Complete bond lengths and bond angles, anisotropic thermal parameters, and calculated hydrogen coordinates are deposited as Supporting Information.

Computational Details. Single-point density functional theory (DFT) calculations were carried out on the triplet state of the dimers of A and B as they are in their X-ray molecular structures (C_i symmetry). The high and low temperature structures yielded qualitatively similar results. The Amsterdam density functional (ADF) program[33] developed by Baerends and co-workers was used.[34] The Vosko−Wilk−Nusair parametrization[35] was used for the local density approximation (LDA) with gradient correction for exchange (Becke 88)[36] and correlation (Perdew 86).[37] Relativistic corrections were added using the ZORA (zeroth order regular approximation) scalar Hamiltonian.[38] The atom electronic configurations were described by a triple-ξ Slater-type orbital (STO) basis set for H 1s, C, N, O 2s and 2p, and Cl 3s and 3p augmented with a 3d single-ξ polarization function for C, N, O, and Cl, and with a 2p single-ξ polarization function for H. A double-ξ STO basis set was used for Pd 4s and Pt 5s, and a triple-ξ STO basis set was used for Pd 4p, 4d, 5s and for Pt 4f, 5p, 5d, and 6s augmented with a single-ξ 5p and 6p for Pd and Pt, respectively. A frozen-core approximation was used to treat the core electrons of C, N, O, Cl, Pd, and Pt.

Scheme 2 Relationship between the RT (—) and LT (····) Unit Cell Parameters

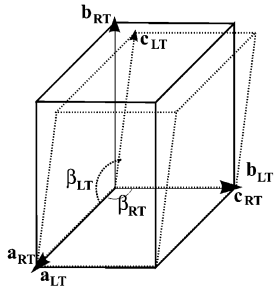

Results and Discussion

Crystal Structures. The crystal structures for both **A** and **B** were solved at 293 K and 120 K, revealing substantial differences. The molecules remain isostructural, but their crystal packing is different for the two temperatures investigated. At room temperature, a monoclinic crystal system is observed with a β angle very close to 90°; we will call it a pseudo-orthorhombic phase. At low temperature, a transition from the pseudo-orthorhombic to the monoclinic phase is found. As shown in Scheme 2, the low temperature phase can be deduced from the room temperature phase using the following matrix (100, 001, 010); i.e., the a parameter is the same, b and c parameters are inverted, and the transition is followed by an opening of the γ_{RT} angle.

For both compounds, the metal atoms adopt the square planar coordination geometry expected for these d^8 metal ions. The ORTEP atomic labeling scheme for compound **A** at room temperature is given in Figure 1. The imino-nitroxide radical is bound to the metal through the imino and the

(30) *Crystal Structure Analysis, (MolEN)*; Enraf-Nonius: Delft, The Netherlands, 1990.
(31) Sheldrick, G. M. *SHELXS-86, Program for the solution of Crystal Structures*; University of Göttingen: Göttingen, Germany, 1985.
(32) Sheldrick, G. M. *SHELXL-93, Program for the refinement of Crystal Structures*; University of Göttingen: Göttingen, Germany, 1993.
(33) *Amsterdam Density Functional program (ADF 2000.02)*; Division of Theoretical Chemistry, Vrije Universiteit: Amsterdam, The Netherlands; http://www.scm.com.
(34) (a) Baerends, E. J.; Ellis, D. E.; Ros, P. *Chem. Phys.* **1973**, *2*, 41. (b) Baerends, E. J.; Ros, P. *Int. J. Quantum Chem.* **1978**, *S12*, 169. (c) Boerringter, P. M.; te Velde, G.; Baerends, E. J. *Int. J. Quantum Chem.* **1988**, *33*, 87. (d) te Velde, G.; Baerends, E. J. *Int. J. Quantum Chem.* **1992**, *99*, 84.
(35) Vosko, S. H.; Wilk, L.; Nusair, M. *Can. J. Phys.* **1980**, *58*, 1200.
(36) (a) Becke, A. D. *J. Chem. Phys.* **1986**, *84*, 4524. (b) Becke, A. D. *Phys. Rev. A* **1988**, *38*, 3098.
(37) Perdew, J. P. *Phys. Rev. B* **1986**, *33*, 8882.
(38) (a) van Lenthe, E.; Baerends, E. J.; Snijders, J. G. *J. Chem. Phys.* **1993**, *99*, 4597. (b) van Lenthe, E.; Baerends, E. J.; Snijders, J. G. *J. Chem. Phys.* **1994**, *101*, 9783. (c) van Lenthe, E.; van Leeuwen, R.; Baerends, E. J. *Int. J. Quantum. Chem.* **1996**, *57*, 281.

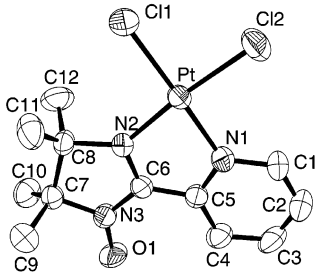

Figure 1. ORTEP view of the molecular structure of **A** at 293 K. Thermal ellipsoids are drawn at the 50% probability level.

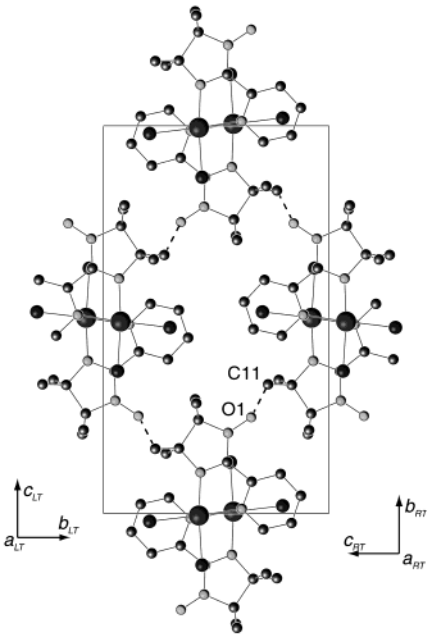

Figure 2. Projection of the crystal structure in the *bc* plane. Dashed lines indicate the shortest intercolumn contacts O1···C11 = 3.30(1) [4.73(2)] and 3.29(1) [4.74(1)] Å for **A** and **B**, respectively.

pyridyl nitrogen atoms forming planar *cis*-MN_2Cl_2 units (M = Pt, Pd). This coordination scheme is in agreement with the weak basic character of the NO group which renders this group difficult to coordinate even to strongly electrophilic metal ions.[14,15] The Pt−Cl and Pt−N average bond distances are 2.295(2) [2.248(8)] and 1.996(6) [1.88] Å, respectively. These values are in agreement with those found for Pt(bpy)-Cl_2.[39] The solid state structure is depicted in Figure 2 as a projection in the *bc* plane. It shows a head to tail arrangement of the molecules in pairs, these dimers being packed in columns parallel to the *a* axis. At 293 K, the intercolumn interactions are characterized by a hydrogen bonding scheme involving the aminoxyl units. The shortest intercolumn distances are found between the oxygen atom of the NO group and the carbon atom of the methyl group of an adjacent column (O1···C11: 3.30(1) [4.73(2)]Å for **A** and 3.293(14) [4.82(3)]Å for **B**) developing, at room temperature only, pseudochains through short NO···H(methyl) contacts (O1···H11C, 2.765 Å for **A**) (see Figure 2). A side view of a column parallel to the *a* direction is depicted in Figure 3. The separations between the mean molecular planes within the pairs, d_1, and between pairs, d_2, are, respectively, 3.651 [3.48] and 4.17 [4.44]Å for **A** and 3.64 [3.48] and 4.19 [4.39]Å for **B**. Unlike the short Pt···Pt distances (3.2−3.4 Å) observed in the linear chains of Pt(II) diimine complexes, such as the red form $Pt(bpy)Cl_2$,[39] the Pt···Pt and Pd···Pd separation found along the columns within and between pairs are 4.124(2) [3.68(2)] Å, 4.402(2) [4.54(2)] Å for **A**, and 4.078(2) [3.69(1)] Å, 4.435(2) [4.696(1)] Å for **B**. Beside the metal−metal distances, the shortest intermolecular distance within a pair is found between the metal of a molecule and the N atom of the pyridyl of the second molecule, Pt···N1 = 3.697(6) [3.61(2)]Å and Pd···N1 = 3.683(7) [3.574(7)]Å for **A** and **B**, respectively (see Figure 3). The phase transition from room temperature (RT) to low temperature (LT) led to reinforced dimer character and very weak intercolumn interactions.

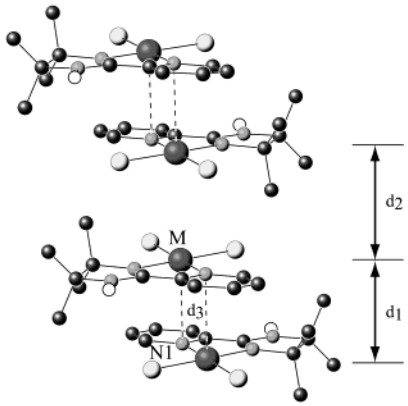

Figure 3. View of the 1D packing along the *a* axis. Dashed lines indicate the shortest intradimer M···N1 contact d_3 = 3.697(6) [3.61(2)] and 3.683-(7) [3.574(7)] Å for **A** and **B**, respectively. The intra- and interdimer separations between the mean molecular planes are d_1 = 3.651(4) [3.48] and 3.64 [3.48] Å and d_2 = 4.17 [4.44] and 4.19 [4.39] Å for **A** and **B**, respectively.

Absorption and Emission Properties. The electronic absorption spectrum of $Pt(IM_2Py)Cl_2$ is strongly perturbed compared to that of $Pt(bpy)Cl_2$, because of the presence of the pyridine-imino-nitroxide ligand IM_2Py. By comparison with $Pt(bpy)Cl_2$,[40] the absorption band with a maximum at 410 nm (ϵ = 6010 M^{-1} cm^{-1}) observed in chloroform solutions has been assigned to a spin allowed MLCT transition associated with the promotion of a platinum d electron into a π^* orbital of the pyridine moiety of IM_2Py. An interesting feature of the $Pt(IM_2Py)Cl_2$ spectrum is the appearance of two less intense absorption bands with two maxima each in the visible region. In chloroform solutions, these maxima are found at 468, 504, 649, and 715 nm with molar extinction coefficients of 3920, 3810, 2000, and 1730 M^{-1} cm^{-1}, respectively. The two visible absorption bands can be clearly associated with the imidazoline-nitroxide moiety.[27,41−43] It should be stressed that these bands in the visible are sensitive to the solvent polarity. The short-

(39) Osborn, R. S.; Rogers, D. *J. Chem. Soc., Dalton. Trans.* **1974**, 1002.
(40) Gidney, P. M.; Gillard, R. D.; Heaton, B. T. *J. Chem. Soc., Dalton Trans.* **1973**, 132.
(41) Ullman, E. F.; Osiecki, J. H.; Boocock, D. G. B.; Darcy, R. *J. Am. Chem. Soc.* **1972**, *94*, 7049−7059 and references therein.
(42) Richardson, P. F.; Kreilick, R. W. *J. Phys. Chem.* **1978**, *82*, 1149−1151.
(43) Oshio, H.; Watanabe, T.; Ohto, A.; Ito, T.; Nagashima, U. *Angew. Chem., Int. Ed. Engl.* **1994**, *33*, 670.

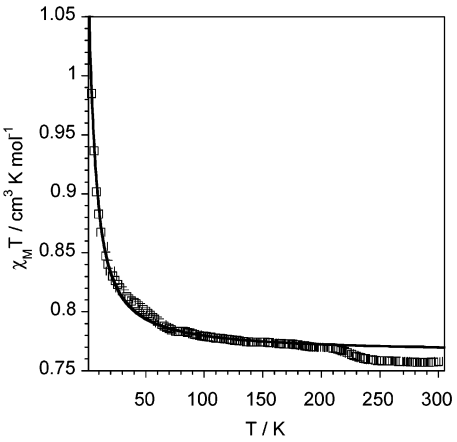

Figure 4. Experimental (□) and calculated (—) temperature dependence of $\chi_M T$ for complex **A**.

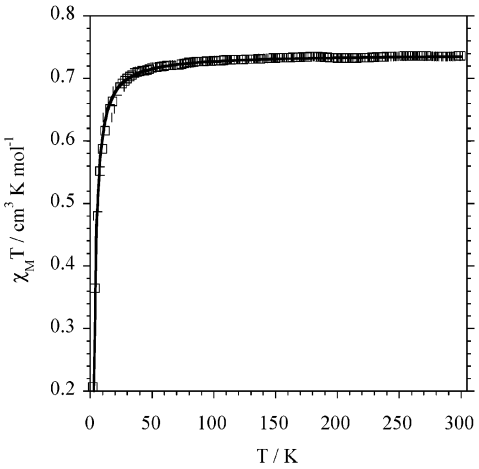

Figure 5. Experimental (□) and calculated (—) temperature dependence of $\chi_M T$ for complex **B**.

wavelength pair is blue-shifted in more polar solvents, appearing at 451 and 484 nm (shift of about 800 cm^{-1}) in acetonitrile, the most polar solvent used. The long-wavelength pair also shows hypsochromic shifts of about 600 cm^{-1} on changing the solvent from chloroform to acetonitrile. Such a solvent effect seems to indicate that the new bands have charge transfer character.[44] Note that the absorption bands observed at 464 and 766 nm for a copper complex [43] and at 650 nm for a vanadyl complex,[45] both bearing the chelating pyridine-imino-nitroxide ligand, have been assigned to MLCT transitions.

The electronic absorption spectrum of $Pd(IM_2Py)Cl_2$ in butyronitrile exhibits (i) in the near-UV, an absorption band with a maximum at 403 nm ($\epsilon = 4630$ M^{-1} cm^{-1}) and a shoulder at 378 nm ($\epsilon = 4040$ M^{-1} cm^{-1}), and (ii) in the visible, a weak and structured absorption band with three peaks at 502 nm ($\epsilon = 730$ M^{-1} cm^{-1}), 537 nm ($\epsilon = 640$ M^{-1} cm^{-1}), and 591 nm ($\epsilon = 460$ M^{-1} cm^{-1}). These bands, which shift to higher energy in more polar solvents, as in the case of $Pt(IM_2Py)Cl_2$, are also assigned to MLCT transitions.

No luminescence has been detected for $Pt(IM_2Py)Cl_2$ and $Pd(IM_2Py)Cl_2$ at room temperature either in solution following excitation at different wavelengths from 300 to 650 nm or in the solid state (laser excitation at 308 nm). However, a very weak emission with a broad band centered at 694 nm was observed only for the Pt complex in butyronitrile glassy solutions at 77 K. This indicates that the emitting state, presumably a MLCT state, is strongly quenched even at 77 K.

Magnetic Properties. The temperature dependence of the molar magnetic susceptibility, χ_M, for compounds **A** and **B** has been investigated in the temperature range 2−300 K. Figures 4 and 5 show the $\chi_M T$ versus T curves drawn for pairs of **A** and **B**, respectively. For the Pd derivative, **B**, the continuous decrease of the $\chi_M T$ value as the temperature is lowered is consistent with dominant antiferromagnetic interactions; conversely, a ferromagnetic behavior is found for **A**. Moreover, the curve for the Pt derivative exhibits a small step around 220 K. We have shown recently that such an anomaly might find its origin in a slight crystal packing reorganization.[47] For the present compounds, the crystal studies revealed as well a different lattice arrangement for the structures at 293 and 120 K (vide supra).

On the basis of the structural information, two pathways for the exchange interactions can be envisaged. One may result from the pair arrangement of the molecules; the second may be operative through the hydrogen bond network involving the aminoxyl units. When considering the crystal structures obtained at 120 K, it appears that the intermolecular NO···H−C have become rather long and no substantial exchange along these contacts is anticipated. Indeed, when the experimental data for the Pt derivative, **A**, were analyzed with a theoretical model for a 1D array of $S = {}^1/_2$ local spins in ferromagnetic interaction,[3,46] the fit to the experimental data below 100 K was poor. These data are, however, perfectly reproduced by a dimer model ($H = -JS_1 \cdot S_2$) suggesting that the dominant exchange interactions take place within the pairs. The best fit to the experimental data in the temperature domain 2−200 K (Figure 4) was obtained for $J = 5.4 \pm 0.1$ cm^{-1} and $zJ' = 0.06$ cm^{-1} ($g = 2.00$, fixed). The parameter zJ' accounts for the weak interactions that exist between the pairs; they have been considered in the mean-field approximation. The data above 200 K were not taken into account because of the modification of the crystal arrangement for the dimers above this temperature. The magnetic behavior for compound **B** was perfectly reproduced by the dimer model as well, and the best fit to the experimental data (Figure 5) yielded $J = -4.25 \pm 0.06$ cm^{-1}.

Obviously, whereas the structural features for the Pt and Pd derivatives **A** and **B** are very much the same, their magnetic properties appear to be rather different. Further information about these compounds was obtained from DFT calculations of the spin density borne by each atom of the

(44) (a) Houlding, V. H.; Miskowski, V. M. *Coord. Chem. Rev.* **1991**, *111*, 145. (b) Tsukahara, Y.; Kamatani, T.; Lino, A.; Suzuki, T.; Kaizaki, S. *Inorg. Chem.* **2002**, *41*, 4363.
(45) Richardson, P. F.; Kreilick, R. W. *J. Phys. Chem.* **1978**, *82*, 1149.
(46) McConnell, H. M. *J. Chem. Phys.* **1963**, *39*, 1919.
(47) Okumura, M.; Mori, W.; Yamagushi, K. *Mol. Cryst. Liq. Cryst.* **1993**, *232*, 35.

Table 3. Selected Atomic Spin Densities Calculated on the Dimers of **A** and **B**[a]

	[Pt(IM$_2$py)Cl$_2$]	[Pd(IM$_2$py)Cl$_2$]
M	0.2337	0.1004
Cl1	0.0000	0.0017
Cl2	0.0891	0.0229
N1	−0.0119	−0.0077
N2	0.3320	0.2968
N3	0.1971	0.2401
O1	0.2810	0.3806
C1	0.0062	0.0023
C2	−0.0211	−0.0087
C3	0.0067	0.0027
C4	−0.0264	−0.0097
C5	0.0149	0.0083
C6	−0.1062	−0.0625
C7	−0.0052	−0.0102
C8	−0.0179	−0.0125
C9	0.0067	0.0207
C10	0.0058	0.0112
C11	0.0045	0.0087
C12	0.0058	0.0169

[a] Triplet state, low temperature X-ray structure.

molecules in the isolated dimers of **A** and **B** considering the low temperature X-ray molecular structures (see computational details). Selected data are given in Table 3. For the Pt derivative, for instance, the highest positive spin density is found as expected on the NO group of the aminoxyl unit. A positive density is also found on the metal ion whereas the N-atom of the pyridine ring displays a weakly negative spin density. Thus, for a pair with short distances between the Pt(II) of one molecule and the pyridine N-atom of the second molecule, an alternation of the sign of the spin density borne by the atoms in close contact is found. This is a favorable situation for a ferromagnetic interaction to occur between the paramagnetic units.[46−47] The same spin distribution holds for the Pd derivative but with much weaker densities found on the atoms as compared to those of the Pt compound. It has been reported before that the intermolecular ferromagnetic exchange mechanism foreseen by the McConnell model may not apply when the alternating spin densities are too small.[48−49] It is very likely that the rather intriguing differences found in the magnetic properties of compounds **A** and **B** are related to the actual spin population on the adjacent atoms. Thus, for the Pt derivative for which substantial spin densities are found on both the metal and N-atoms, a McConnell type exchange mechanism accounts for a ferromagnetic interaction between the two open-shell molecules of a pair. This mechanism does not apply for the Pd derivative because of the much less significant spin population on the considered atoms and antiferromagnetic interactions become dominant.

A further difference in the magnetic behavior of compounds **A** and **B** concerns the step apparent around 220 K on the $\chi_M T$ versus T plot for **A** whereas no anomaly is observed for **B**. As already mentioned, such a step might be the signature for a sudden crystal lattice reorganization.[46] The X-ray structure analyses performed at 293 and 120 K show indeed that such a reorganization takes place for both compounds. For compound **A**, this subtle reorganization has a visible effect on the exchange interactions as exhibited by the $\chi_M T$ versus T plot; clearly, the ferromagnetic contribution is enhanced below 220 K. It is interesting to notice that the structural modification for **B** is not revealed by its magnetic properties.

Concluding Remarks

This work was initiated in order to explore the coordination chemistry of the imino nitroxide radical bearing ligand 2-(ortho-pyridyl)-4,4,5,5-tetramethylimidazoline-1-oxyl toward Pt(II) and Pd(II) metal ions. To the best of our knowledge, compound **A** is the first platinum complex involving such a ligand.

The magnetic properties studies performed on these compounds revealed ferromagnetic intermolecular interactions to be operative for the Pt derivative whereas an overall antiferromagnetic behavior was found for its Pd counterpart. Both compounds undergo a phase transition at low temperature; nevertheless, they remain isostructural in the whole temperature range explored. DFT calculations suggest that the apparent metal effect might be related to the spin density distribution. Indeed, whereas for both **A** and **B** an alternation of the sign of the spin densities on the closest atoms of two adjacent molecules is found, the densities obtained for the Pd derivative are much weaker than those for the Pt compound. Thus, the ferromagnetic intermolecular interaction foreseen by the McConnell exchange mechanism applies for the Pt compound, but the smaller spin density values for the Pd derivative might prevent it from taking place.

The study of the absorption and emission spectra of compound **A** revealed only a weak luminescence for **A** at 77 K, indicating that the emitting state is strongly quenched. The finding of this luminescence is promising for the design of new {M(II) imino-nitroxide radical} complexes with improved photophysical features, in order to achieve materials which couple both magnetic and optical properties. Current investigations are being carried out toward this direction.

Acknowledgment. This work was supported by the CNRS, l'Université de Rennes 1, SABIC, and King Fahd University of Petroleum and Minerals, Saudi Arabia (Grant SABIC 99/6), and the TMR Research Network of the European Union ERB-FMRX-CT-98-0181 entitled "Molecular Magnetism: from Materials toward Devices".

Supporting Information Available: X-ray crystallographic files, in CIF format, for **A** and **B** at room temperature and low temperature. This material is available free of charge via the Internet at http://pubs.acs.org.

IC0255813

(48) Michaut, C.; Ouahab, L.; Bergerat, P.; Kahn, O.; Bousseksou, A. *J. Am. Chem. Soc.* **1996**, *118*, 3610.
(49) Zheludev, A.; Barone, V.; Bonnet, M.; Delley, B.; Grand, A.; Ressouche, E.; Rey, P.; Subra, R.; Schweizer, J. *J. Am. Chem. Soc.* **1994**, *116*, 2019.